AIP Journal of Applied Physics

Plasmonic enhancement of spontaneous emission from wide-linewidth emitters with nanostrip metallic waveguide

Chao Zhang, Xue Feng, Kaiyu Cui, and Yidong Huang

Citation: J. Appl. Phys. **114**, 053105 (2013); doi: 10.1063/1.4817417
View online: http://dx.doi.org/10.1063/1.4817417
View Table of Contents: http://jap.aip.org/resource/1/JAPIAU/v114/i5
Published by the AIP Publishing LLC.

JOURNAL OF APPLIED PHYSICS 114, 053105 (2013)

Plasmonic enhancement of spontaneous emission from wide-linewidth emitters with nanostrip metallic waveguide

Chao Zhang, Xue Feng,[a)] Kaiyu Cui, and Yidong Huang[b)]
Department of Electronic Engineering, State Key Laboratory of Integrated Optoelectronics, Tsinghua University, Beijing 100084, China

(Received 31 January 2013; accepted 18 July 2013; published online 5 August 2013)

Purcell factor of a nanostrip plasmon waveguide is evaluated via a full integration form of Fermi's golden rule and power dissipation spectrum. Purcell factor is dramatically increased with narrower strip width, corresponding to the tight confinement in the ultrasmall gap region. Furthermore, inclusion of energy distribution among useful and lossy modes would reduce the Purcell factor severely, yet the enhancement range could be broadened and the tolerance of emission linewidth strengthened. Although the dissipation issue remains serious near the resonant frequency, it is shown that wide-linewidth emitters in the off-resonance region could also be effectively enhanced with nanostrip waveguide, suggesting a promising path to practical integrated emitters. © *2013 AIP Publishing LLC*. [http://dx.doi.org/10.1063/1.4817417]

I. INTRODUCTION

Surface plasmon polariton (SPP) is a transverse magnetic (TM)-polarized electromagnetic wave coupling to the collective oscillation of free charge carriers at metal-dielectric interface.[1,2] In principle, SPP could yield large density of state (DOS) and small mode volume near the resonant frequency, which is beneficial in boosting the spontaneous emission (SE) of active materials, known as Purcell effect.[3,4] Generally, the Purcell factor (*PF*) is proportional to the ratio of quality factor (Q) over the mode volume of a cavity. However, the well-known spectral broadening effect of practical emitters suggests that chasing a high-Q cavity alone cannot obtain a high *PF*, and generalized discussions on emitter/quantum dot (QD)-cavity interaction have been delivered in Refs. 5 and 6. In plasmonic domain, gap-mode plasmonic waveguide provides such a platform where ultrasmall mode volume could be achieved with meticulous design, implying the possibility of ultrahigh *PF*, especially for wide-linewidth emitters.[7,8] Recent experimental demonstration of strong enhancement by gap-mode SPP[9] witnessed a much higher *PF* value than previously obtained in planar plasmonic waveguides or metallic gratings/crystals.[10–13] However, in such a system where the emitter is located in close proximity to metallic materials, the energy distribution among useful modes and lossy modes should be considered.[13] This effect could be serious in designing plasmonic-enhanced emitters. Therefore, model of *PF* via considering the impact of emission linewidth, propagation loss and energy distribution should be built regarding gap-mode plasmonic waveguide.

In this work, the plasmonic enhancement of a nanostrip metallic waveguide is investigated. As the most popular figure of merit, *PF* is first calculated from a full integration form of Fermi's golden rule, where both the emission linewidth of active material and spectral broadening of DOS are taken into account. The dispersion relation and electromagnetic field distribution are solved by effective index method and finite element method (FEM), respectively. It is found that when the strip width is narrowed down to tens of nanometers, the Q of the waveguide remains stable near the resonant frequency, while the field could still be well confined in the waveguide. Subsequently, the impact of energy distribution is evaluated by power dissipation spectrum (PDS). The ratio of energy coupled into SPP mode is estimated as $\sim$50% (and smaller near the resonant frequency). Modified *PF* is obtained by multiplying *PF* spectrum and energy ratio of SPP mode. Particularly, when the strip width is 20 nm, the *PF* could be as high as $\sim$110 near the resonant frequency of 3.4 eV. Moreover, our result shows that when the energy distribution is considered, the *PF* peak becomes wider and the maximum value of *PF* degrades much slower with broadening emission linewidth. This strong tolerance suggests a promising application of the nanostrip waveguide to the plasmonic enhancement of wide-linewidth emitters.

II. PURCELL FACTOR OF NANOSTRIP METALLIC WAVEGUIDE

The considered nanostrip plasmon waveguide, as shown in Figure 1, is very similar to the microstrip line for high frequency circuits.[14] The structure consists of a metal strip and a metal substrate separated by a dielectric thin layer with uniformly embedded emitters. Also, this waveguide could be split into a metal-insulator-metal (MIM) plasmon waveguide and two metal-dielectric-air waveguides, and the SPP mode of interest is confined in the gap beneath the metal strip to interact effectively with the active material. The confinement is achieved vertically by the metal-dielectric interfaces and horizontally by the different effective refractive index of the core and surrounding sections. We shall see later that this confinement is very strong even when the width of the strip is only tens of nanometers, which leads to ultrasmall mode volume and eventually ultrahigh *PF*.

[a)]Electronic mail: x-feng@tsinghua.edu.cn
[b)]Electronic mail: yidonghuang@tsinghua.edu.cn

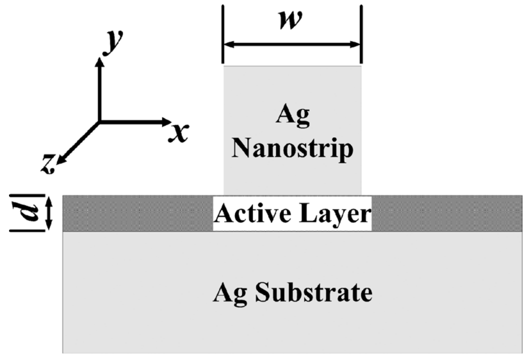

FIG. 1. Schematic nanostrip plasmon waveguide and reference coordinate system. The width of the nanostrip and the thickness of the active layer are denoted by w and d, respectively.

It is well known that both the emission linewidth of active material and the spectral broadening of DOS would affect the Purcell enhancement. In this work, the *PF* of the nanostrip waveguide is obtained in a practical manner as we previously employed.[12] Starting from full form of Fermi's golden rule, the SE rate of active material is

$$\Gamma_{SPP}(\omega_0) = \int_0^{\infty} \sum_k \frac{2\pi}{\hbar^2} |\langle f|\boldsymbol{d}\cdot\boldsymbol{E_k}|i\rangle|^2 \cdot \rho(\omega-\omega_k) \times l(\omega-\omega_0) d\omega. \quad (1)$$

Here, the emission spectrum $l(\omega - \omega_0)$ is assumed to be homogeneously broadened and could be expressed as the normalized Lorentzian shape function $l(\omega-\omega_0) = \frac{\Delta\omega}{2\pi}/[(\omega-\omega_0)^2 + (\Delta\omega/2)^2]$, where ω_0 and $\Delta\omega$ denote the central emission frequency and linewidth, respectively.[15] $\rho(\omega - \omega_k)$ is the DOS spectrum introduced by the propagation loss of SPP mode and is also expressed as Lorentzian shape $\rho(\omega-\omega_k) = (\omega_k/2\pi Q_k)/[(\omega-\omega_k)^2 + (\omega_k/2Q_k)^2]$, where ω_k and Q_k are the frequency and quality factor corresponding to mode k, respectively. Q_k can be calculated from the dispersion relation as $Q_k = \omega_k/\alpha v_g$, where $\alpha = 2\mathrm{Im}[k]$ is the energy dissipation rate and v_g is the group velocity.[16] $\langle f|\boldsymbol{d}\cdot\boldsymbol{E}_k|i\rangle$ is the emission matrix element of the emitter. The emission dipole $\boldsymbol{d}$ is assumed to be randomly oriented to the electric field and an average factor of 1/3 is taken as $|\boldsymbol{d}\cdot\boldsymbol{E_k}| = \frac{1}{3}|\boldsymbol{d}|^2 \cdot |\boldsymbol{E_k}|^2$. $\boldsymbol{E_k}$ should be normalized to the half-quantum of zero point fluctuations within a prepared space $V = L_xL_yL_z$, with stored field energy $\frac{1}{8\pi}\int\int\int_V \frac{\partial(\varepsilon\omega)}{\partial\omega}\cdot E_k^2(x,y)dxdydz$.[4] Since only the coupling efficiency is concerned here, the model could be simplified in 2D case, where the effective mode volume is proportional to L_z.[8] In the cross-section, the electromagnetic field is confined in the gap so that the transverse integration can be extended to infinity. Thus the stored energy can be rewritten as $\frac{L_z}{8\pi}\int\int_\infty \frac{\partial(\varepsilon\omega)}{\partial\omega}\cdot E_k^2(x,y)dxdy$. Further, for propagating mode on z direction, $k_x = 0$, $k = k_z$, and hence $\Delta k = \Delta k_z = 2\pi/L_z$. By summing up over k-space we can obtain the overall decay rate. Then with the well-known SE rate in bulk material $\Gamma_0 = \frac{4nd^2\omega_0^3}{3\hbar c^3}$, the *PF* can be expressed as

$$PF(\omega_0|x,y) = 1 + \frac{\Gamma_{SPP}(\omega_0)}{\Gamma_0} = 1 + \frac{\pi c^3}{n\omega_0^2}\sum_k H(\omega_k)\cdot\rho(\omega-\omega_k)\cdot l(\omega-\omega_0)\Delta k. \quad (2)$$

Here $H(\omega_k) = \frac{|E_k^2(x,y)|}{\int_{-\infty}^{+\infty}\int_{-\infty}^{+\infty}\frac{\partial(\varepsilon\omega)}{\partial\omega}\cdot E_k^2(x,y)dxdy}$ describes the confinement of the electromagnetic field. n is the refractive index of the dielectric and c is the light speed in vacuum. Approximating the sum over k-space to the integration of ω_k by multiplying dk/dω_k, the full integration expression of *PF* is as follows:

$$PF = 1 + \frac{\pi c^3}{n\cdot\omega_0^2}\int_0^\infty\int_0^\infty H(\omega_k)\cdot\rho(\omega-\omega_k)l(\omega-\omega_0)\frac{dk}{d\omega_k}d\omega_k d\omega. \quad (3)$$

As a concrete example, the metal is chosen as silver with permittivity of $\varepsilon(\omega) = 1 - \omega_p^2/(\omega^2 - i\omega\gamma)$, where $\omega_p = 7.9$ eV and $\gamma = 0.06$ eV,[13] and the dielectric layer SiN_x with permittivity of 4.0. The emitter is taken as Si-QD embedded in a 10 nm-thick SiN_x film, with reported ω_0 in 1.7–4.0 eV.[17–20] For such a waveguide with a thin active layer, fabrication is challenging yet achievable with sputtering/chemical vapor deposition (CVD) and electron-beam (EB) lithography.[21] Furthermore, typical process for the growth of Si-QD requires high temperature annealing (>700 °C),[17] which would damage the metal layer. Fortunately, low temperature growth (<300 °C) of active SiN_x without annealing process has been reported[18] and could be employed in the fabrication of our waveguide.

Effective index method and FEM simulation are employed to obtain the dispersion relation and field distribution required by the *PF*. First, the waveguide is approximated to an MIM waveguide sandwiched by two identical metal-dielectric-air planar waveguides. The effective refractive index of the MIM waveguide is higher than that of the planar ones so that the electromagnetic field can be confined in the central area. The calculated dispersion curve and propagation length (defined as 1/Im[k]) of nanostrip plasmon waveguide with gap thickness $d = 10$ nm and strip width $w = 20$–200 nm are shown in Figures 2(a) and 2(b), respectively. It can be found that dispersion curves corresponding to different strip widths converge near the resonant frequency, suggesting similar confinement mechanism of each waveguide. Also, an increased propagation length with narrowing strip width is noted. However, the dissipation in the resonance region is still so severe that large propagation length ~1 μm can only be possibly obtained below 2.5 eV. Second, the field distribution is solved by FEM simulation and numerical integration is performed for the calculation of effective mode volume.

Purcell factor for Si-QD with central emission frequency from 2.0 to 3.7 eV is calculated while $\Delta\omega$ is fixed at 152 meV as a middle value from Ref. 20. *PF*s are averaged within the entire gap region and the results are shown in Figure 3(a). It can be seen that the peak value of *PF* is

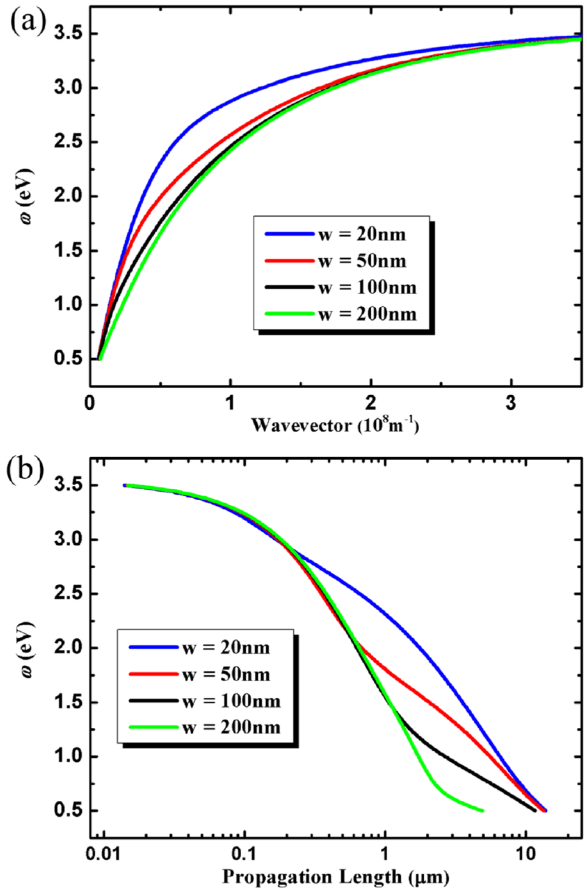

FIG. 2. (a) Dispersion relation of nanostrip plasmon waveguide with strip width ranging from 20 to 200 nm. (b) Propagation length (1/Im[k]) of nanostrip plasmon waveguide.

achieved around resonant frequency of 3.4 eV. For strip width larger than 100 nm, the calculated *PF* value is very close to previous reports of MIM waveguide.[8] However, the maximum value of *PF* shows an evident increase with narrowing strip width. Particularly, the maximum *PF* is larger than 240 when the strip width is 20 nm.

In detail, as shown in Figure 3(b), the Q of ∼57 is nearly constant around the resonant frequency within the strip width range of 20–200 nm. This moderate quality factor is due to the propagation loss of plasmon waveguide. On the other hand, however, the ultrahigh *PF* obtained here is attributed to the tightly confined electromagnetic field in the gap region. Calculated $H(\omega_k)$ are shown in Figure 3(c). It is clearly seen that $H(\omega_k)$ increases when strip width decreases. Especially, $H(\omega_k)$ for strip width of 20 nm is one order higher than that of 200 nm, which consequently results in the ultrahigh *PF*. However, for even smaller strip width, fundamental mode of the nanostrip waveguide would cut off and the field would broaden away, resulting in a slightly improved Q value together with a notably increased mode volume.

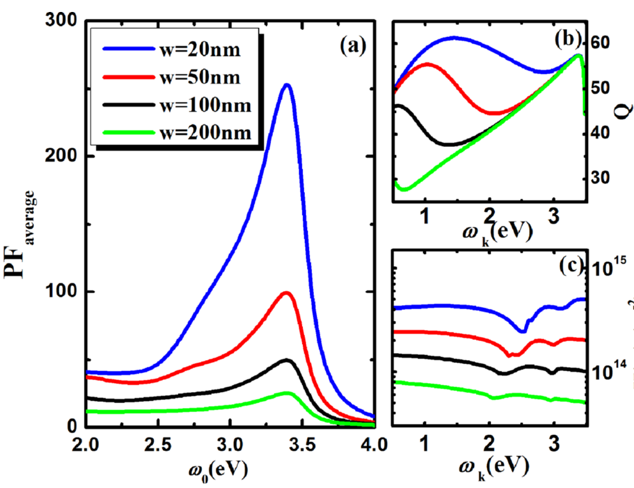

FIG. 3. (a) Original *PF* spectra, (b) Q, (c) $H(\omega_k)$ with strip width = 20–200 nm, respectively.

III. MODIFICATION OF *PF* SPECTRUM VIA PDS

In a lossy system as the nanostrip waveguide, the emission energy of dipole is only partially coupled into useful modes. Therefore, the ratio of energy directed to useful mode (radiation and SPP mode) to that of the lossy mode needs to be considered. Here we adapt a classical model developed in Ref. 22 and widely used in Refs. 8, 13, and 23. In a simplified case, we consider an MIM waveguide with a dielectric layer of 10 nm. The emitter with isotropic polarization is located beneath one metal slab with a distance of 1/4 of the gap thickness, i.e., 2.5 nm. The emission of the dipole is mediated by the electromagnetic field reflected by the interfaces of metal and dielectric, and would behave differently for different modes, denoted by normalized in-plan wavevector $u_{\parallel}$ (normalized to free-space light wavevector with the same frequency). The power dissipation spectrum for $\omega = 3.0$ eV is plotted in the inset of Figure 4(a). The main peaks around the effective refractive index (n_{eff}) of SPP mode represent the coupling to SPP mode. Wavevector interval of 0–1 represents the radiation and $n_{eff} \sim \infty$ stands for lossy surface modes, mainly consisting of the electron scattering loss in the metal, which is even more closely bonded to the metal-dielectric interface and thus has higher in-plan wavevector than SPP modes.[13,24] By calculating the area beneath the lines in each wavevector range, the energy distribution among the three modes can be obtained. Here the three intervals are divided by $u_{\parallel} = 1$ and $u_{1/2}$, i.e., the wavevector where power dissipation rate is reduced to half of its maximum value. Here the dividing point of $u_{1/2}$ is chosen to distinguish the contribution of SPP mode and lossy surface mode as reasonable estimation, since the boundary between these two modes is not so distinct in itself. Figure 4(a) is the power dissipation rate for different emission frequencies and $u_{\parallel}$, denoted by grayscale map. Via selective integration, as shown in Figure 4(b), dissipation rates of SPP and lossy modes both increase rapidly near the resonant frequency, while radiative rate remains very low. The energy ratio of SPP mode is denoted by blue line in Figure 4(b). A broad peak can be observed around 2.7 eV, corresponding to higher efficiency in off-resonance region.

Considering energy distribution in this structure, modified *PF* spectra of nanostrip waveguide are obtained by multiplying the original *PF* spectra with the energy ratio of SPP mode. As shown in Figure 5, maximum *PF* value of

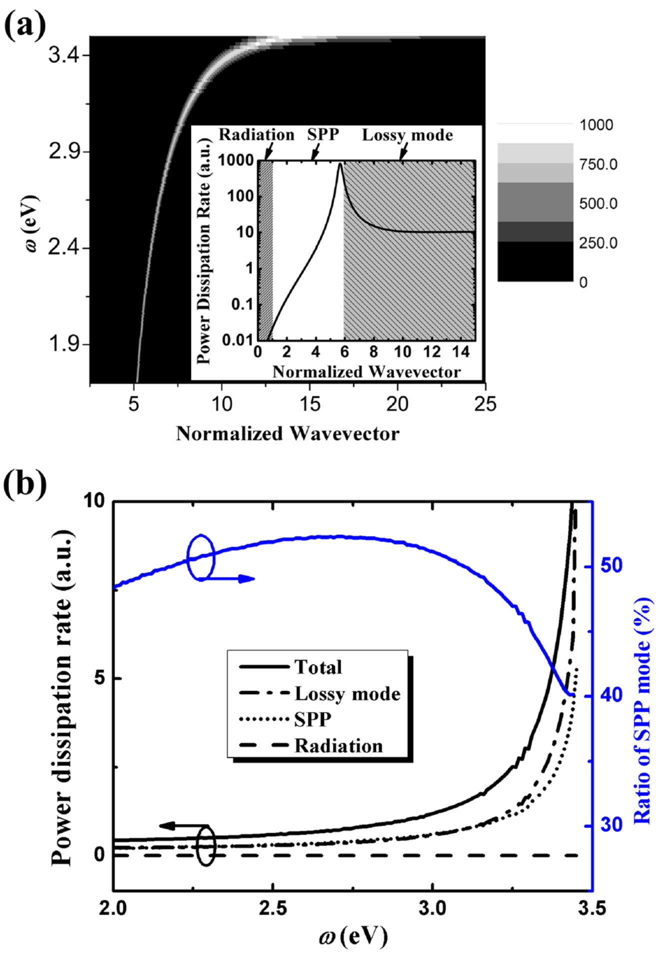

FIG. 4. (a) Power dissipation rate corresponding to different frequency and normalized in-plan wavevector. Inset: Power dissipation spectrum for $\omega = 3.0\,\mathrm{eV}$, wavevector intervals represent radiation, SPP, and lossy surface wave, respectively. (b) Total dissipation rate, coupling into radiation, SPP, and lossy mode are denoted by solid, dashed, dotted, and dashed-dotted lines, respectively. Ratio of SPP mode is represented by blue line.

nanostrip waveguide with $w = 20\,\mathrm{nm}$ is reduced to 110. Meanwhile, the enhancement region is much wider, i.e., *PF* is less reduced in the off-resonance frequency ($PF = 50$ at $\omega = 2.78\,\mathrm{eV}$). Via this model, we combined the impact of spectral broadening of DOS and energy distribution among different modes in a simplified and convenient way. Nevertheless, MIM waveguide is adopted instead of the

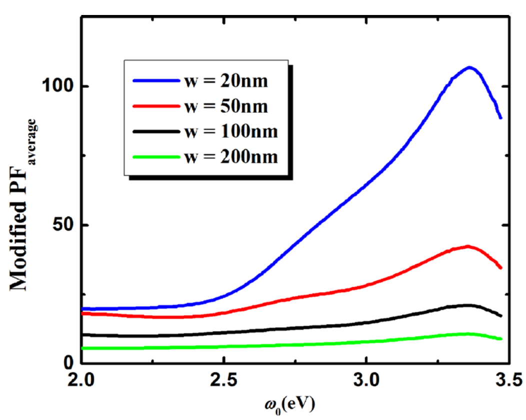

FIG. 5. Modified *PF* spectra for strip width ranging from 20 to 200 nm.

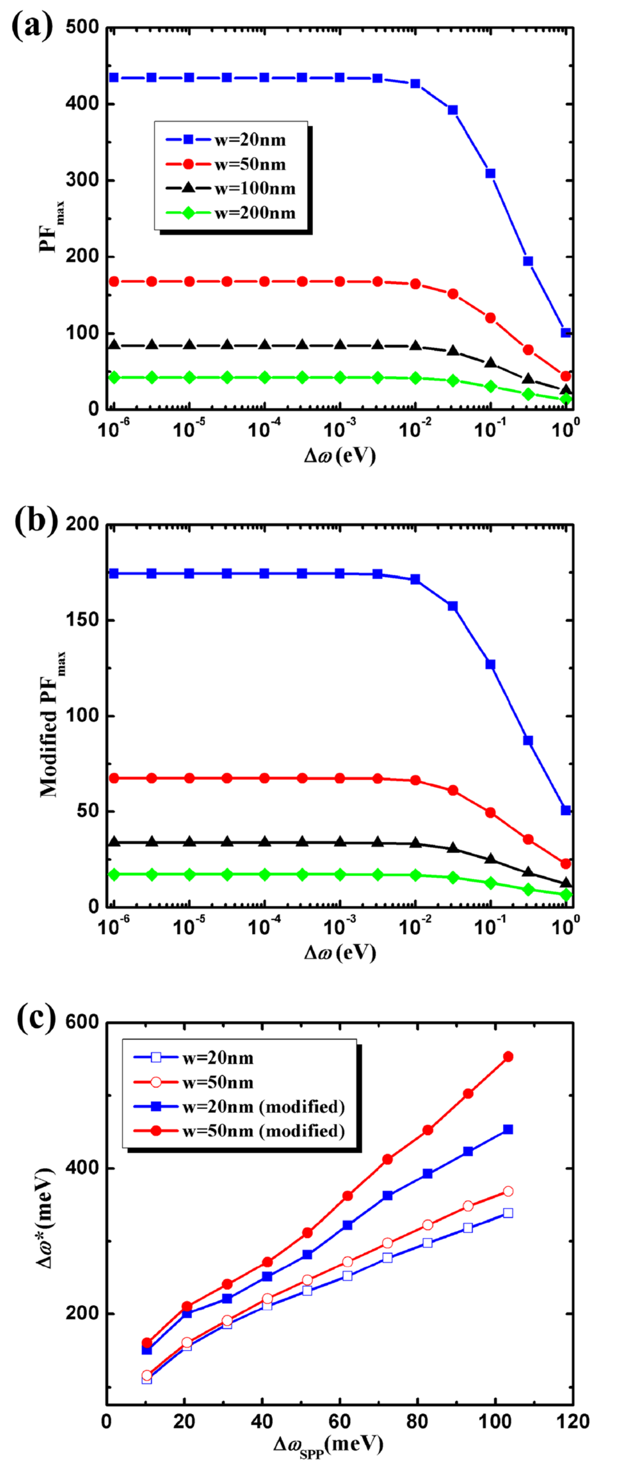

FIG. 6. Evolution of maximum value of *PF* spectra with different emission linewidth, evaluated with (a) simplified model and (b) modified model. (c) Critical emission linewidth with different plasmonic linewidth, calculated by both models.

nanostrip waveguide as estimation. Therefore, slightly different *PF* could be expected in more detailed evaluations.

The simulation result for wide strip waveguide is very close to the measured value (∼12) in Ref. 25. On the one hand, the gap was thicker and mode volume thus larger, which would lower the *PF* value. On the other hand, the emission linewidth ∼20 meV is much smaller than that of Si-QD used in our model, which would alleviate the spectral broadening effect. More recently, $PF \sim 1000$ was experimentally reported by Russell *et al.*, with a metallic nanorod rather than a strip placed above the active layer.[9] Note that the nanorod is equivalent to an even smaller strip width, which would give rise to the higher PF observed in the experiment. Also, the emitters in the experiment are located within 2 nm above the 10 nm spacing layer. Since SPP is a surface wave, this structure would provide a more effective interaction between emitters and the SPP field.

Furthermore, the impact of emission linewidth on the PF is investigated with both the original and modified model. By varying $\Delta\omega$ from 1 μeV to 1 eV, achievable PF with different strip widths are plotted in Figures 6(a) and 6(b). It can be found that the peak PF values are reduced by the energy ratio of the SPP mode at resonant frequency. This is reasonable since the PF spectra are much sharper than the peak of SPP energy ratio spectrum. For both cases, PF degrades severely only when $\Delta\omega$ is larger than 100 meV, and it should be noted that PF degrades more slowly after considering the energy distribution. To quantitatively evaluate this effect, we define the critical emission linewidth $\Delta\omega^*$ as the linewidth where PF is reduced to half of its maximum. The evolution of $\Delta\omega^*$ with SPP linewidth ranging from 10 to 100 meV is calculated by multiplying certain values to the quality factor of SPP mode. The results of w = 20 nm and 50 nm for both models are shown in Figure 6(c). Quasi-linear relations between $\Delta\omega^*$ and $\Delta\omega_{SPP}$ are observed, which indicates that the broad linewidth of SPP mode offers the adaptability to wide-linewidth emitters. As discussed in our previous work,[12] the dissipation of plasmon waveguide would be beneficial for wide-linewidth emitters due to the enlarged integration range. What's more, the $\Delta\omega^*$ of modified model is larger than that of original model, suggesting that the tolerance to wide-linewidth emitters is stronger. This effect should also be taken into account while designing plasmonic-enhanced emitters, especially for wide-linewidth emitters and broad-band enhancement.

IV. CONCLUSIONS

In conclusion, we calculated the PF of nanostrip metallic waveguide via a full integration form of Fermi's golden rule, while the impact of emission linewidth, DOS broadening, and energy distribution among different modes is considered. The electromagnetic field is found to be tightly confined in the gap region, which attributes to an ultrasmall mode volume. Energy distribution between useful and lossy modes is investigated with power dissipation spectrum. As estimated, ultimate PF spectra are obtained by multiplying original PF with energy proportion of SPP mode. The energy distribution issue would reduce PF value while provide a stronger tolerance to wide-linewidth emitters, in addition to the same effect of DOS broadening. This effect should be considered in designing broadband-enhanced wide-linewidth emitters. Particularly, in the off-resonance region, high $PF \sim 50$ and lower dissipation (propagation length $\sim 1\,\mu$m) could be expected, which is promising for a practical integrated emitter.

ACKNOWLEDGMENTS

This work was supported by the National Basic Research Program of China (No. 2011CBA00608, 2011CB301803, 2011CBA00303, and 2010CB327405) and the National Natural Science Foundation of China (Grant Nos. 61036011 and 61036010). The authors would like to thank Dr. Wei Zhang, Dr. Fang Liu, and Dr. Keyong Chen for their valuable discussions and helpful comments.

[1] W. L. Barnes, A. Dereux, and T. W. Ebbesen, Nature **424**, 824 (2003).
[2] A. V. Zayatsa, I. I. Smolyaninovb, and A. A. Maradudinc, Phys. Rep. **408**, 131 (2005).
[3] E. M. Purcell, Phys. Rev. **69**, 37 (1946).
[4] I. Gontijo, M. Boroditsky, E. Yablonovitch, S. Keller, U. K. Mishra, and S. P. DenBaars, Phys. Rev. B **60**, 11564 (1999).
[5] M. P. van Exter, G. Nienhuis, and J. P. Woerdman, Phys. Rev. A **54**, 3553 (1996).
[6] T. Suhr, N. Gregersen, M. Lorke, and J. Mork, Appl. Phys. Lett. **98**, 211109 (2011).
[7] E. J. R. Vesseur, F. J. G. de Abajo, and A. Polman, Phys. Rev. B **82**, 165419 (2010).
[8] Y. C. Jun, R. D. Kekatpure, J. S. White, and M. L. Brongersma, Phys. Rev. B **78**, 153111 (2008).
[9] K. J. Russell, T.-L. Liu, S. Y. Cui, and E. L. Hu, Nature Photon. **6**, 459 (2012).
[10] H. Iwase, D. Englund, and J. Vučković, Opt. Express **18**(16), 16546 (2010).
[11] X. Feng, F. Liu, and Y. D. Huang, J. Lightwave Technol. **28**(9), 1420 (2010).
[12] X. Feng, K. Y. Cui, F. Liu, and Y. D. Huang, Appl. Phys. Lett. **101**, 121102 (2012).
[13] W. L. Barnes, J. Lightwave Technol. **17**(11), 2170 (1999).
[14] D. D. Grieg and H. F. Engelmann, Proc. IRE **40**(12), 1644 (1952).
[15] *Spontaneous Emission and Laser Oscillation in Microcavities*, edited by H. Yokoyama and K. Ujihara (CRC, New York, 1995), Chap. 8.
[16] Y. Gong and J. Vučković, Appl. Phys. Lett. **90**, 033113 (2007).
[17] B. H. Kim, C. H. Cho, T. W. Kim, N. M. Park, G. Y. Sung, and S. J. Park, Appl. Phys. Lett. **86**, 091908 (2005).
[18] T. W. Kim, C. H. Cho, B. H. Kim, and S. J. Park, Appl. Phys. Lett. **88**, 123102 (2006).
[19] E. V. Rogozhina, D. A. Eckhoff, E. Grattonb, and P. V. Braun, J. Mater. Chem. **16**, 1421 (2006).
[20] J. Valenta, R. Juhasz, and J. Linnros, Appl. Phys. Lett. **80**, 1070 (2002).
[21] H. T. Miyazaki and Y. Kurokawa, Phys. Rev. Lett. **96**, 097401 (2006).
[22] R. R. Chance, A. H. Miller, A. Prock, and R. Silbey, J. Chem. Phys. **63**, 1589 (1975).
[23] J. Barthes, G. C. des Francs, A. Bouhelier, J. C. Weeber, and A. Dereux, Phys. Rev. B **84**, 073403 (2011).
[24] G. W. Ford and W. H. Weber, Phys. Rep. **113**(4), 195–287 (1984).
[25] Y. Gong, S. Yerci, R. Li, L. D. Negro, and J. Vuckovic, Opt. Express **17**(23), 20642 (2009).